



OPEN The chemotherapy agent doxorubicin induces CNS expression of Ascl1, a regulator of adult neurogenesis and differentiation

Christi Anne S. Ng¹, Morgan Pedus², Madeline F. Lee¹, Lawrence F. Kromer¹, Jeanne Mandelblatt³ & G. William Rebeck¹✉

Cancer-related cognitive impairment (CRCI) is a common side effect of cancer and its treatments. Cancer chemotherapy has been associated with hippocampal dysfunction and memory impairment. We investigated the effects of one chemotherapy agent, doxorubicin, on the transcription factor Ascl1 and proliferation of stem cells in the brain. We used an inducible mouse model designed to express TdTomato in Ascl1-lineage cells. Five to six-month-old Ascl1-CreERT2:ROSA mice were treated peripherally with a single dose of either doxorubicin (10 mg/kg) or DMSO control ($n = 9$ per group, $n = 4-5$ per sex). We analyzed brains of mice that had been exposed to doxorubicin for 2 weeks and had induced Ascl1 expression after the first week. We used immunostaining of neurogenesis stage specific markers to evaluate the doxorubicin effects on neuronal differentiation in the dentate gyrus of the hippocampus. Overall, doxorubicin significantly increased Ascl1 expression by 81% at this time point. As measured by Ascl1 double stains with Sox2, GFAP, and NeuroD1, doxorubicin-treated mice experienced an increase in Ascl1-mediated neural proliferation compared to control. A similar significant increase in the number of Ascl1-expressing cells (by 146%) after doxorubicin treatment was observed in the gray matter of the cerebral cortex. Thus, rather than leading to the loss of developing neurons, we found that a single dose of doxorubicin increased their appearance and progression, suggesting that hippocampal losses from chemotherapies may require greater and more sustained damage.

Keywords Chemotherapy-related cognitive impairment, CRCI, Cancer, Neurogenesis, Ascl1, Dentate gyrus

As rates of cancer survivorship improve, the number of patients burdened with long-term side effects of cancer and its treatments continues to increase. Up to 75% of cancer survivors commonly report transient or long-term symptoms of memory loss, slowed processing speed, impaired executive function, and attention difficulties, most commonly after chemotherapy¹⁻⁵. Despite a growing body of literature, mechanisms underlying this constellation of symptoms, known as cancer chemotherapy-related cognitive impairment (CRCI), remain poorly defined^{4,6}.

In particular, both clinical and pre-clinical studies have linked CRCI-related memory loss with hippocampal dysfunction and impaired neurogenesis⁶⁻¹⁶. Neurogenesis in the adult brain includes neural stem cells in the dentate gyrus subgranular zone of the hippocampus differentiating into new neurons¹⁷. Alterations in the adult hippocampus, a vital structure for memory and learning, are strongly associated with cognitive dysfunction in a broad array of neurological conditions¹⁸⁻²⁰. Chemotherapy has been linked in a few pre-clinical studies with a decline in neural progenitor cell proliferation and survival, along with behavioral deficits of hippocampal mediated memory²¹⁻²⁴.

However, the effects of the chemotherapeutic agent doxorubicin, commonly used to treat a range of tumors, on neurogenic depletion have been inconsistent. Using a variety of markers, some studies have found no effects

¹Department of Neuroscience, Georgetown University, 3970 Reservoir Rd, NW, Washington, DC 20007, USA.

²Molecular Biology, Cell Biology, and Biochemistry Department, Brown University, Providence, RI, USA.

³Department of Oncology, Georgetown University, Washington, DC, USA. ✉email: gwr2@georgetown.edu

on cell proliferation or cell maturation after doxorubicin treatment^{1,21,25}. Three studies found that multiple treatments of doxorubicin impaired spatial memory and hippocampal memory processing in rodent models, as well as reduced expression of doublecortin (DCX; a late neuronal marker) and 5-bromo-2'-deoxyuridine incorporation into DNA (BrdU; for labeling of dividing cells)^{9,26,27}. However, one study found that four weekly doxorubicin treatments did not significantly affect BrdU labeling 1 week later²⁸. Another found that a single dose of doxorubicin did not impact DCX or Ki-67 (a marker of intermediate progenitor proliferation) expression 3 or 16 weeks post treatment¹⁰. Investigating the detrimental stimuli affecting neural stem cell survival and differentiation may require a more systematic assessment of the signaling pathways regulating neurogenic lineages^{18,20,29}.

Adulthood neurogenesis consists of a precise series of steps: proliferation, differentiation, maturation, and migration¹⁷. The neural stem cell populations in the dentate gyrus pass through multiple developmental stages coordinated by the activity of transcription factor networks and signaling mechanisms³⁰. Achaete-scute homolog 1 (Ascl1), a proneural bHLH transcription factor, is a critical regulator of adult stem cell proliferation, neuronal differentiation, and subtype specification^{31–33}. Ascl1 is first expressed in activated intermediate progenitors then down-regulated as neurons differentiate, balancing cell cycle re-entry and cell cycle progression^{31,32,34}. Ascl1 is essential in normal neural cell reprogramming and differentiation; variable levels of Ascl1 can result in unequal distributions of neuronal subtypes, as well as inappropriate differentiation and cell cycle exit³⁴. However, the effect of Ascl1 possibly mediating the effects of chemotherapy on brain functions has not been addressed.

We used an Ascl1 reporter mouse line that allowed us to test this hypothesis. We exposed mice to a single dose of the chemotherapeutic agent doxorubicin and followed the Ascl1-expressing cells through several stages of proliferation, differentiation, and morphological changes. We found that within 2 weeks of exposure to doxorubicin, Ascl1 expression was induced, and cells containing markers of various stages of neural differentiation were elevated. Over time, this dysregulation of neurogenesis related to Ascl1 expression may deplete neural stem cells needed for continued regeneration of hippocampal neurons. Chemotherapy agents such as doxorubicin could cause some aspects of CRCI through this chronic, Ascl1-related effect to the neural stem cells of the hippocampus.

Results

We treated female and male Ascl1-CreERT2:ROSA mice at 5–6 months of age with a single dose of 10 mg/kg doxorubicin or DMSO vehicle. One week later, we induced Ascl1-TdTomato expression by four consecutive days of tamoxifen injections. Two weeks after doxorubicin treatment, we euthanized mice and imaged Ascl1-positive cells through fluorescent immunostaining of TdTomato (Fig. 1A). As expected for this tamoxifen-inducible mouse model^{35,36}, TdTomato labeled cells of various morphologies throughout the brain. Cells were prominently

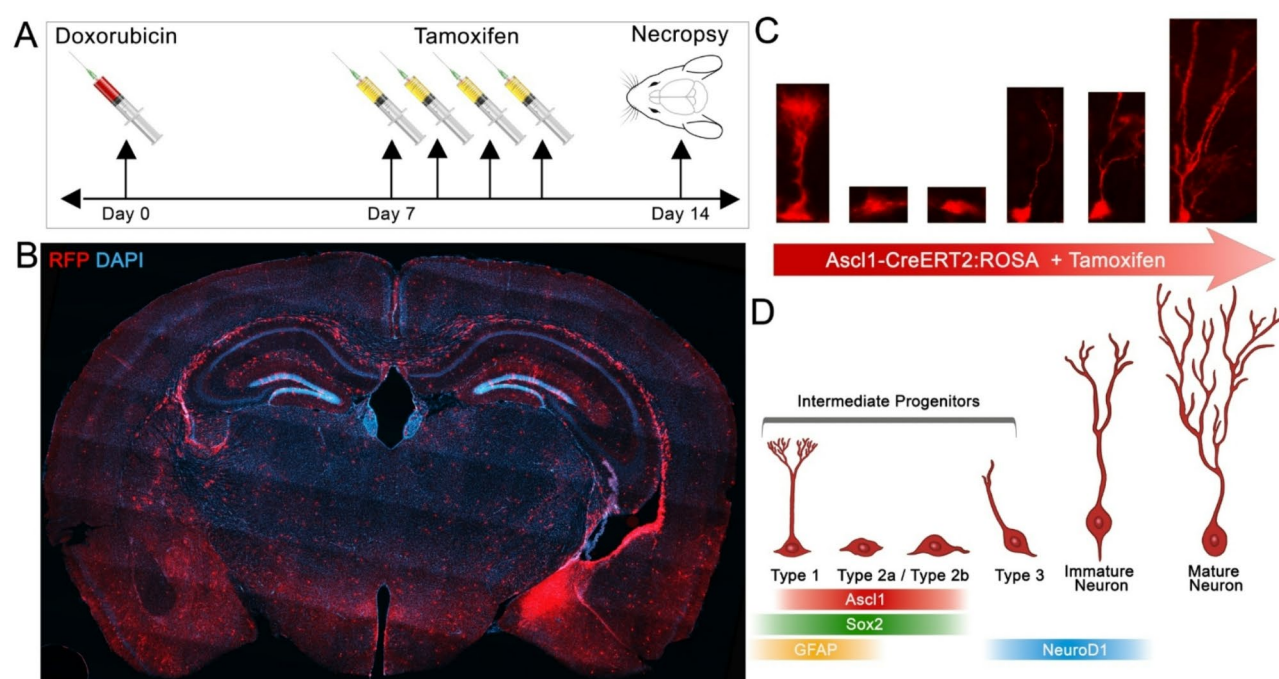


Fig. 1. Distribution of Ascl1-positive neurons in the mouse brain. (A) Experimental timeline of doxorubicin treatment and tamoxifen induction. (B) Stitched image of a coronal brain section showing Ascl1-TdTomato expression detected with the rabbit RFP antibody (red) with a DAPI counterstain (blue). (C) Representative images of Ascl1-TdTomato expression in subgranular zone neurogenic cells. (D) Schematic of morphological maturation of hippocampal neurons and stage specific markers.

found in the white matter and in the hippocampus (particularly the dentate gyrus); a more diffusely distributed number of cells were present in the cerebral cortex, subcortical regions, and white matter (Fig. 1B).

Doxorubicin increases Ascl1 expression in the dentate gyrus

We initially focused on the dentate gyrus in our analysis of the effects of doxorubicin on TdTomato immunoreactivity. As expected^{31,35,36}, the TdTomato marker identified cells in the subgranular zone with a variety of morphologies, including Type-1 cells with a bushy soma (Radial Glia-like Cells), Type 2 cells with irregular shape, and maturing neurons with developing dendritic arbors (Fig. 1C,D). The pattern of TdTomato staining was similar across sexes and treatment conditions (Fig. 2A). However, the amount of Ascl1 expression was affected by treatment condition: doxorubicin treatment led to statistically significant increases in the mean intensity of TdTomato expression by 81% ($*p=0.041$ $t=2.225$, $df=16$) and percent area coverage by 36% ($*p=0.02$, $t=2.573$, $df=16$) (Fig. 2B,C). There was no significant sex difference in the increase in TdTomato immunostaining after doxorubicin treatment between females (109%) and males (57%). A similar pattern of the effect of doxorubicin was seen in an increase in the number of cells in the subgranular zone of the dentate gyrus expressing Ascl1-TdTomato (33%), but this difference did not reach statistical significance ($p=0.074$, $t=1.91$, $df=16$). There was no statistically significant difference in the observed increase in TdTomato-positive cell numbers after doxorubicin exposure in females compared to males (Fig. 2D). These data demonstrate that doxorubicin treatment induced higher levels of Ascl1-neural proliferators in the dentate gyrus.

Doxorubicin affects other measures of neurogenesis in the dentate gyrus

To characterize the stage-specific changes in Ascl1-lineage cells observed in Fig. 2, we co-immunostained with morphological markers of different stages of adult neurogenesis: Sox2, NeuroD1, and GFAP.

Sox2 is expressed early in neural stem cell proliferation and persists through both type-1 and type-2 progenitor cells of the dentate gyrus granule layer^{19,35}. We observed Sox2-positive cells throughout the hippocampus

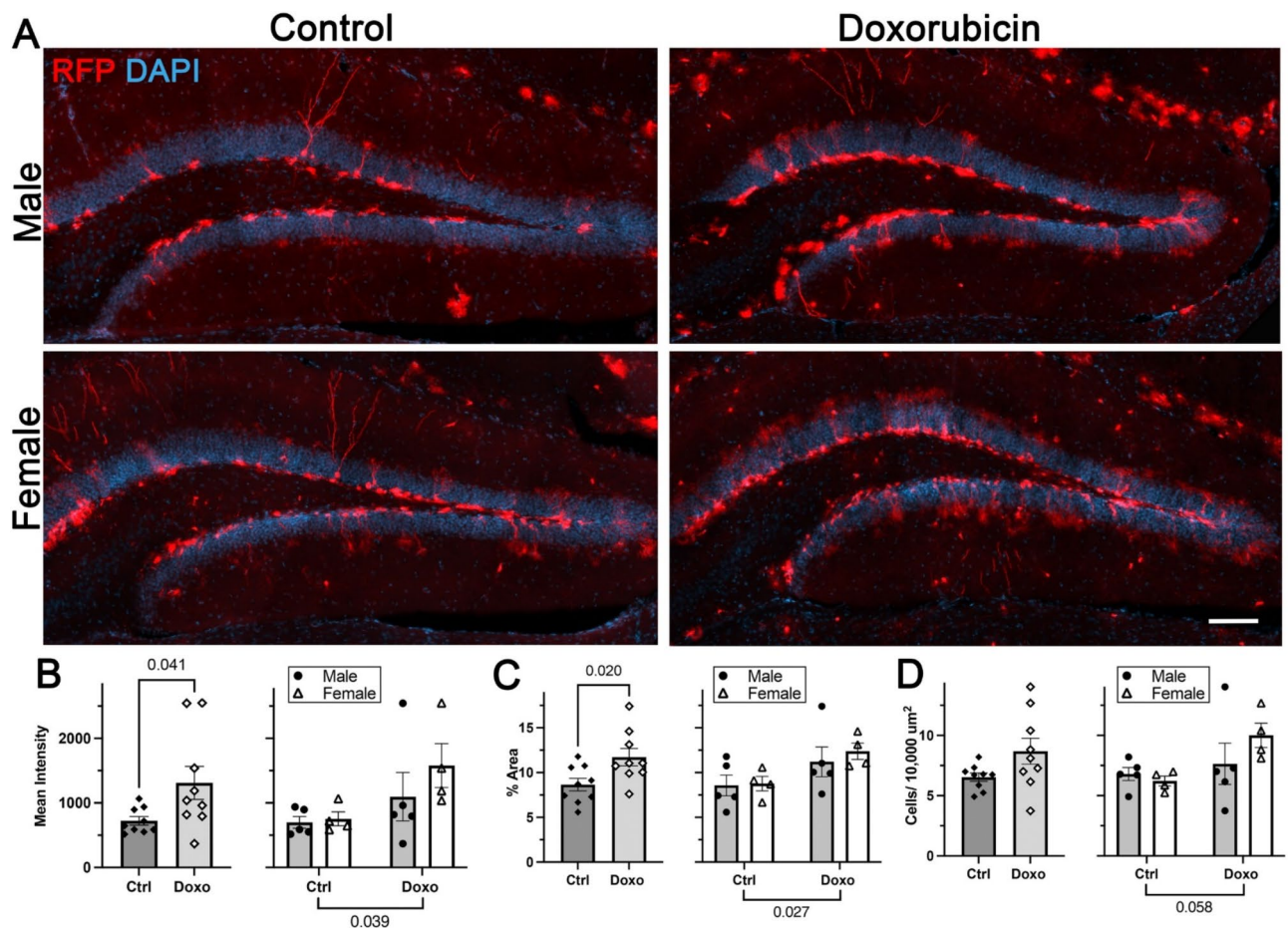


Fig. 2. Doxorubicin induction of Ascl1-expression in the dentate gyrus. (A) Representative stitched images of the dentate gyrus from doxorubicin and control treated male and female mice. Dentate gyri were analyzed for Ascl1-TdTomato (red) (B) mean intensity, (C) percent area coverage, and (D) TdTomato-positive cell counts. Unpaired T-tests and Two-way ANOVAs were used to assess outcomes from doxorubicin and sex. Bar graphs represent the mean \pm SEM, $n=4-5$ animals per group, ~ 4 slices per brain, ~ 3 images at 20X magnification per slice (magnification bar = 100 μm).

(Fig. 3A), most numerous in the dentate gyrus subgranular zone, but also in many neurons throughout the hippocampus (Fig. 3C,D). Doxorubicin significantly increased Sox2 immunoreactivity (percent area coverage) in the dentate gyrus across both sexes (Fig. 3E; $*p=0.048$, $t=2.144$, $df=16$). There were no differences in Sox2 mean intensity nor cell numbers in the area around the subgranular zone (data not shown). There were no differences observed in the effects of doxorubicin treatment on Sox2-positive cell numbers in female mice (27%) compared to male mice (21%). In the subgranular zone, Sox2 immunoreactivity co-localized with the cell

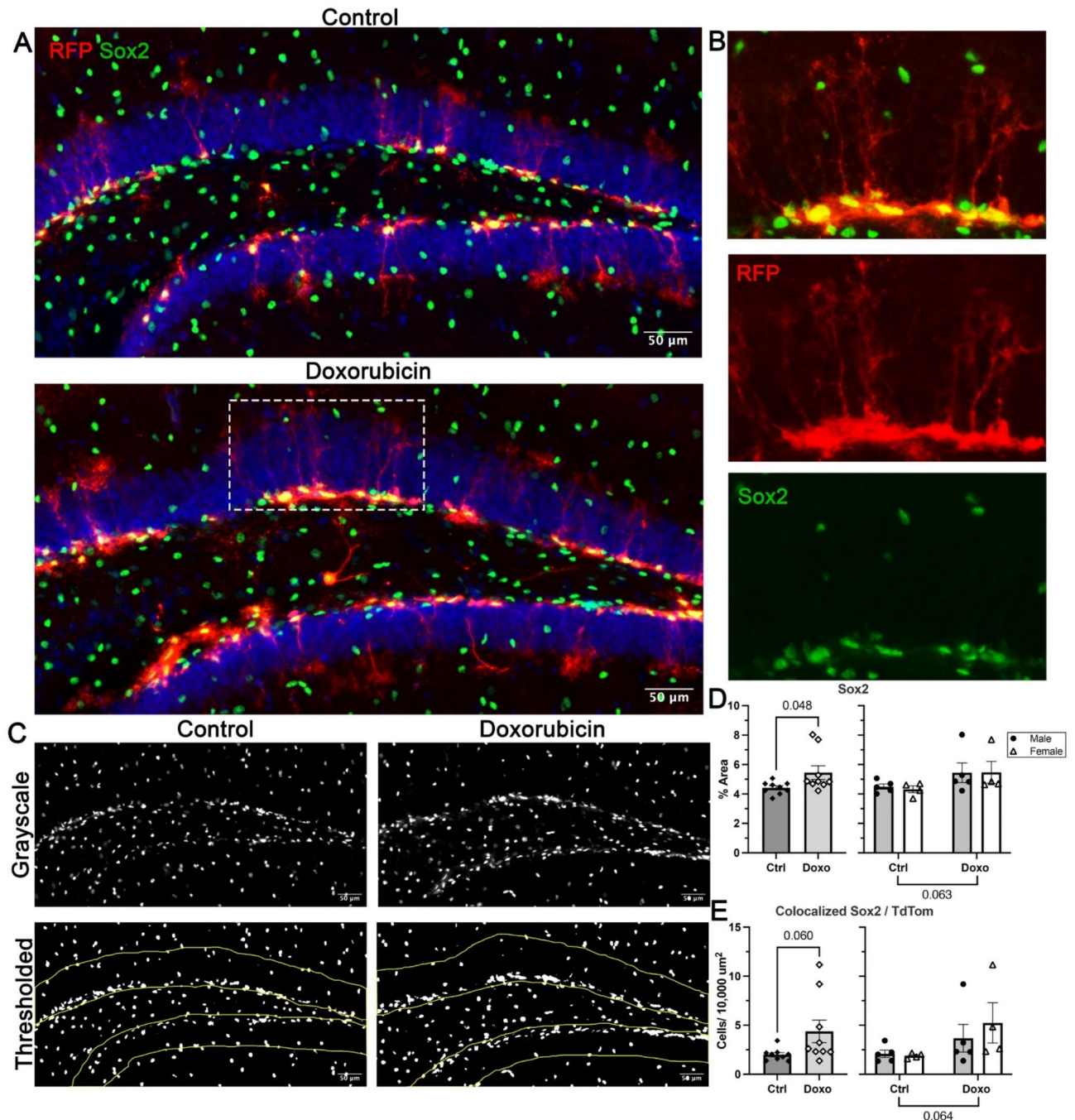


Fig. 3. Doxorubicin induction of Sox2 expression in the dentate gyrus. (A) Representative 10X composite images of TdTomato (red), Sox2 (green), and DAPI (blue) from control and doxorubicin treated mice. (B) Cropped image (boxed area) illustrating quantification based on number of colocalized cells (yellow). (C) Example of 10X grayscale images of Sox2 channel and thresholding performed for percent area analysis within the dentate gyrus ROI (yellow outline) in control and doxorubicin treated brains. (D) Quantification of percent area coverage of Sox2 channel and (E) counts of colocalized cells per 10,000 μm^2 . Unpaired T-tests and Two-way ANOVAs used to assess outcomes from doxorubicin and sex. Bar graphs represent the mean \pm SEM, $n=4-5$ animals per group, ~ 4 slices per brain, 1 image at 10X magnification per slice.

bodies of TdTomato-positive cells (Fig. 3B). In counts of Sox2 positive cells that co-localized with TdTomato, we observed a non-significant increase of 120% with doxorubicin treatment (vs. controls) overall (Fig. 3F, $p=0.06$, $t=2.023$, $df=16$). There were no differences in the doxorubicin-stimulated increase in Sox2-TdTomato colocalized cell counts between female mice (180%) and male mice (76%). Thus, doxorubicin increased Sox2 expression overall and in Ascl1-lineage neural progenitors of the dentate gyrus.

GFAP expressing cells in the subgranular zone of the dentate gyrus mark the glial-to-neuron conversion of stem cells³⁷. GFAP immunostaining identified astrocyte-like cells throughout the hippocampus, but also identified a population of subgranular zone cells with one main, apical process that extends through the dentate gyrus (Fig. 4A,B). We first quantified the total number of cells co-expressing GFAP and TdTomato in the subgranular zone of the dentate gyrus to assess the effects of doxorubicin (Fig. 4A,D). Doxorubicin treated mice had a two-fold increase in the total number of colocalized cells compared to control mice ($*p=0.01$, $t=2.922$, $df=16$). There were no statistically significant differences in measures of doxorubicin increases based on sex (150% in females and 66% in males), perhaps due to the relatively small numbers of mice per sex^{4,5}. Next, we

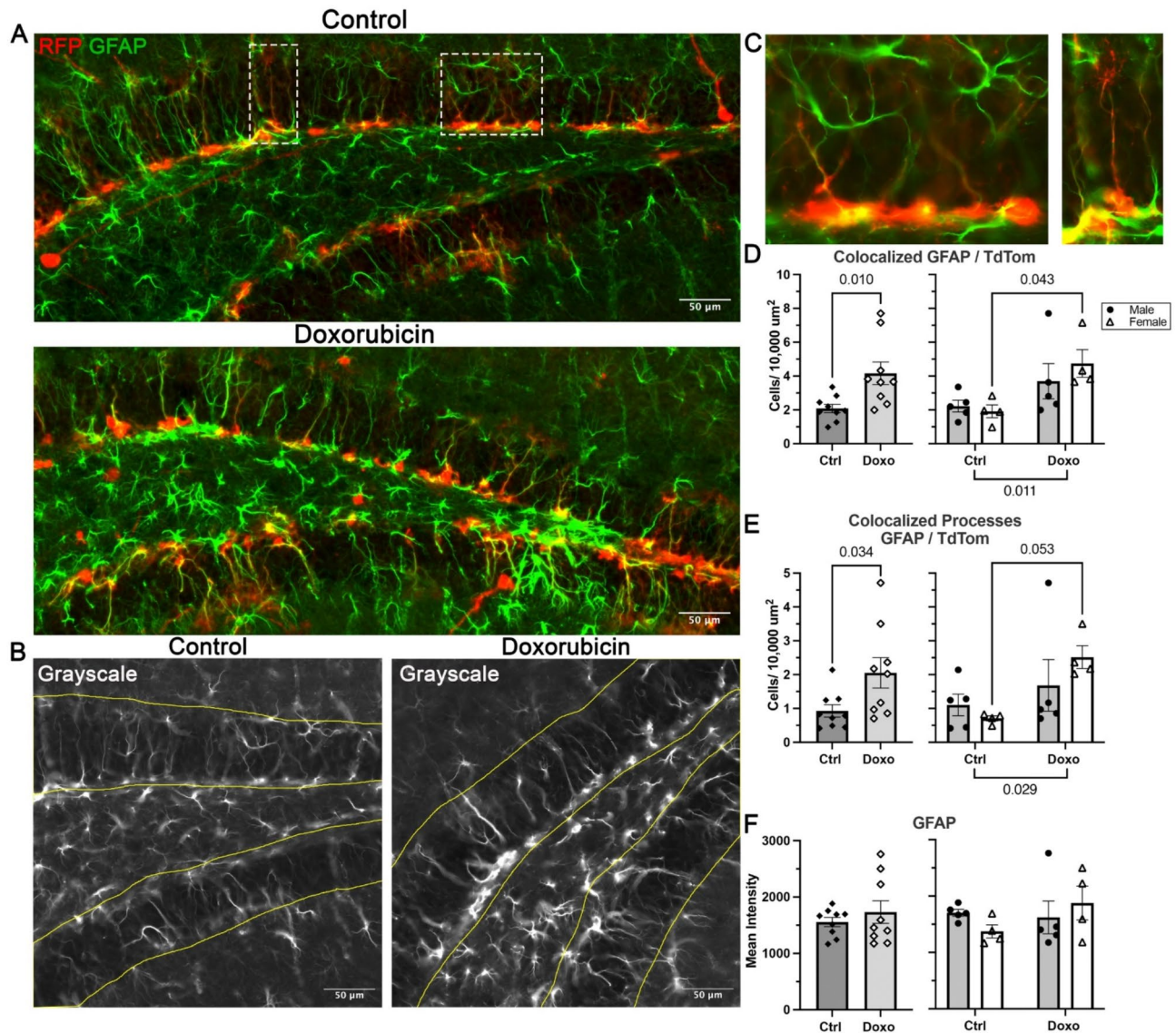


Fig. 4. Doxorubicin increases the number of GFAP-positive/Ascl1-positive cells in the dentate gyrus. (A) Representative 10X composite image of TdTomato (red), GFAP (green), and colocalization (yellow) from control and doxorubicin treated brains. (B) Example of 20X grayscale image of GFAP channel used for mean intensity analysis within the dentate gyrus ROI (yellow outline) of control and doxorubicin treated mice. (C) Cropped images (boxed areas) of colocalized cell types. (D) Quantification of total number of colocalized cells and (E) cells with colocalized processes per 10,000 μm² and (F) mean intensity of GFAP within the dentate gyrus. Unpaired T-tests and Two-way ANOVAs used to assess outcomes from doxorubicin and sex. Bar graphs represent the mean ± SEM, $n=4-5$ animals per group, ~4 slices per brain, ~3 images at 20X magnification per slice.

assessed the quantity of Ascl1-TdTomato cells colocalizing with GFAP in a single cell process extending from the cell body (Fig. 4B,E). This approach allowed us to characterize the chemotherapeutic response of Ascl1-lineage radial glial progenitors (type-1 progenitors) separate from the role of Ascl1 in glial cell development. In the dentate gyrus granule layer, the number of cells with colocalized TdTomato-positive/GFAP-positive processes significantly increased by 120% with doxorubicin treatment in both sexes combined ($*p = 0.029$, $t = 2.320$, $df = 16$). Similar to the findings with all TdTomato-positive/GFAP-positive cells, there were non-significant increases in females (250%) as well as males (50%). When we included all GFAP cells in the dentate gyrus, which included mature astrocytes, there were no differences in GFAP mean intensity after doxorubicin treatment (Fig. 4C,F). The presence of these astrocytes limited our ability to accurately count which cells were developing neurons and which were differentiated astrocytes; therefore, we did not analyze the effects of doxorubicin on GFAP-positive cell numbers or total GFAP expression in the analyzed regions. Together, our results suggest that doxorubicin promotes an Ascl1-mediated increase of GFAP intermediate progenitors in the subgranular zone.

NeuroD1 is first expressed in late type-2 cells and persists into postmitotic immature neurons, and thus is a marker of more mature developing neurons³⁸. We quantified the number of NeuroD1 cells that co-localized with TdTomato. We found that doxorubicin treatment was associated with a trend towards a significant increase in the number of NeuroD1 and TdTomato co-expressing cells by 61% compared to control (Fig. 5A,C; $p = 0.052$, $F^{1,14} = 4.495$). In doxorubicin-treated females, although there were over 2 times the number of NeuroD1-TdTomato cells in doxorubicin-treated females compared to controls ($*p = 0.035$), there was overall not a significant difference between sexes. Total coverage of the dentate gyrus by NeuroD1 immunoreactivity was not affected by doxorubicin treatment (Fig. 5B,D).

Doxorubicin increased Ascl1 expression in the cortex

Next, we assessed Ascl1-TdTomato immunoreactivity in the cortex, based on the distribution of Ascl1-TdTomato seen there (Fig. 1). While adult neurogenesis occurs in the granule layer of the dentate gyrus, Ascl1 is a differentiation control factor expressed in other brain cells as well³⁹. Thus, we measured the quantity of TdTomato-positive cells in the cortex to evaluate whether the upregulation of Ascl1-lineage cells was specific to hippocampal neuronal subtypes or occurred throughout the brain. Doxorubicin treatment increased Ascl1-TdTomato staining in the cortex (Fig. 6A,B). The cortical staining was in cells with neuronal morphologies (Fig. 6C,E). As in Fig. 1, there was also strong staining in the white matter; these cells displayed glial morphologies (Fig. 6D). Quantification of the number of cells demonstrated increased numbers of Ascl1-TdTomato positive cells by 150% compared to controls across both sexes (Fig. 6F; $*p = 0.008$, $t = 3.004$, $df = 16$). The quantity of positive cells almost tripled with doxorubicin treatment in female mice compared to control females (Fig. 6G; $*p = 0.02$). Thus, doxorubicin treatment was associated with higher levels of cortical Ascl1-lineage cells compared to control, and thus may have effects on non-dividing neurons as well.

Discussion

Cancer chemotherapy has been linked to hippocampal changes through brain imaging and through the learning and memory problems among cancer survivors. These observations raise the possibility that developing neurons in the hippocampus are particularly susceptible to chemotherapy-related damage. In this current preclinical study, we found that a single doxorubicin treatment increased Ascl1 expression in the hippocampus and the cortex 2 weeks after treatment, with consistent findings in each stage of hippocampal neurogenesis (as defined by Sox2, GFAP, and NeuroD1 markers). Thus, rather than leading to the loss of developing neurons of the adult dentate gyrus, we found that, at early times of exposure, doxorubicin increased their progression.

Our model is that an early effect of chemotherapy in the CNS is induction of expression of the Ascl1 transcription factor. Ascl1 is necessary for cellular development and differentiation³⁵ but requires the presence of other stimuli to drive increased neurogenesis and gliogenesis⁴⁰. We observed doxorubicin-induced expression of Ascl1 not only in the dentate gyrus subgranular zone, but also in cortical cells⁴¹, particularly in the white matter, where this expression is important from oligogenesis⁴². Doxorubicin has a limited ability to cross the blood brain barrier and thus these effects are likely the result of indirect actions, such as induction of peripheral inflammation²⁵. We hypothesize that after repeated or more intense peripheral damages from chemotherapeutic agents, further stimulation of Ascl1-related pathways may drive its effects on stem cell differentiation; over time, this proliferation may lead to exhaustion of the stem cells, accounting for loss of hippocampal volume in CRCI^{43–45}.

The downstream neurotoxic action of chemotherapeutic agents with low blood brain barrier permeability is poorly understood^{21,22,46}. Doxorubicin effects on hippocampal neurogenesis have been inconsistent, with some studies indicating neurogenic depletion and others showing no changes after doxorubicin treatment^{9,10,26–28}. These discrepancies may be due to differences in study design, methods for visualizing neurogenesis, or variability in the doxorubicin blood-brain barrier permeability^{21,22}. Our study provides an in-depth examination of the early stages in the cascade affecting neural stem cell proliferation. In proliferating cells of the adult hippocampus, Ascl1 is responsible for balancing the cells that are maintained as progenitors with those that undergo differentiation; these cells are identifiable as activated Type 1 and Type 2a neural progenitors^{31,35}.

In the Ascl1-CreERT2:ROSA model, tamoxifen administration elicits the TdTomato labeling in Ascl1 expressing cells, with persistent TdTomato labeling of Ascl1 lineage cells up to 180 days post treatment^{36,47}. For proliferation to begin, quiescent radial glial-like cells (early Type 1 cells) require Ascl1 for activation and specification of neuron fate, as identifiable by double labeling of TdTomato with GFAP³¹. As the TdTomato-positive cells proliferate, both Type1 and Type 2a/2b can be identified by co-labeling with Sox2. Our analysis of TdTomato double labeling with Sox2 or GFAP indicated that doxorubicin not only upregulated Ascl1-lineage cells overall, but also upregulated the specification of Type 1 cells and the proliferation of intermediate progenitors. While we observed an upregulation of Sox2 independent of Ascl1, GFAP expression alone was not

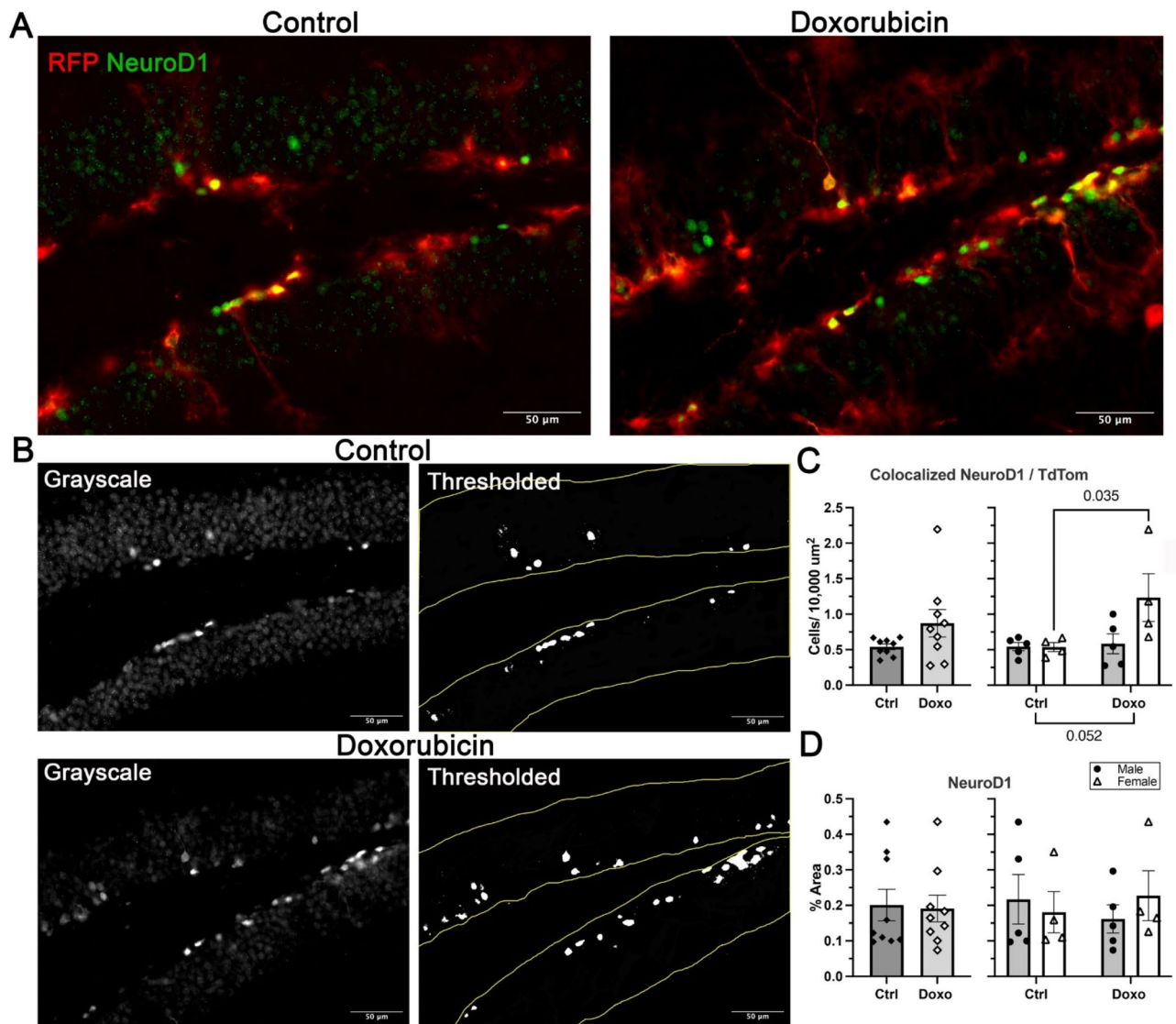


Fig. 5. Doxorubicin increases NeuroD1-Ascl1 cells in the dentate gyrus of female mice. **(A)** Representative 20X composite images of TdTomato (red), NeuroD1 (green), and colocalization (yellow) in doxorubicin or control treated female mice. **(B)** Example of 20X grayscale images of NeuroD1 channel and thresholding performed for percent area analysis within the dentate gyrus ROI (yellow outline) of control and doxorubicin treated brains. **(C)** Quantification of counts of colocalized cells per 10,000 μm^2 and **(D)** percent area coverage of NeuroD1 within the dentate gyrus. Unpaired T-tests and Two-way ANOVAs used to assess outcomes from doxorubicin and sex. Bar graphs represent the mean \pm SEM, $n = 4$ –5 animals per group, ~ 4 slices per brain, ~ 3 images at 20x magnification per slice.

affected by doxorubicin. These results suggest the upregulation was specific to the initiation of proliferation and neuronal subtype specification, while astrocytic activity was unchanged.

While Ascl1 expression is typically down regulated as neurogenesis proceeds, the Cre recombinase model allows for lineage tracing of cells that had expressed Ascl1 during the tamoxifen treatment, and the TdTomato marker persists beyond Ascl1 expression. Thus, our analysis of NeuroD1 co-labeling with TdTomato permitted characterization of the cells transitioning into Type 3 cells and immature granule neurons³⁵. We again observed an upregulation of TdTomato double labeled cells (although the total number of NeuroD1 cells was unchanged). Consistent with our other results, doxorubicin increased the NeuroD1 marker of neural survival and maturation in the cells that had earlier expressed Ascl1. Thus, doxorubicin promoted the appearance and development of dentate gyrus stem cells within 1–2 weeks after exposure. These early changes indicate that there are disruptions to hippocampal homeostasis at early stages of exposure to chemotherapy agents.

We found that the significant increase in Ascl1 intensity in the dentate gyrus was paired with a (non-significant) increase in the number of Ascl1-positive cells. These data are consistent with an increase in Ascl1 expression in developing neural cells but also an increase in their number. Previous research has associated chemotherapeutics with depletion of neurogenesis and proliferation markers²⁴. Since overexpression of Ascl1 correlates with a loss

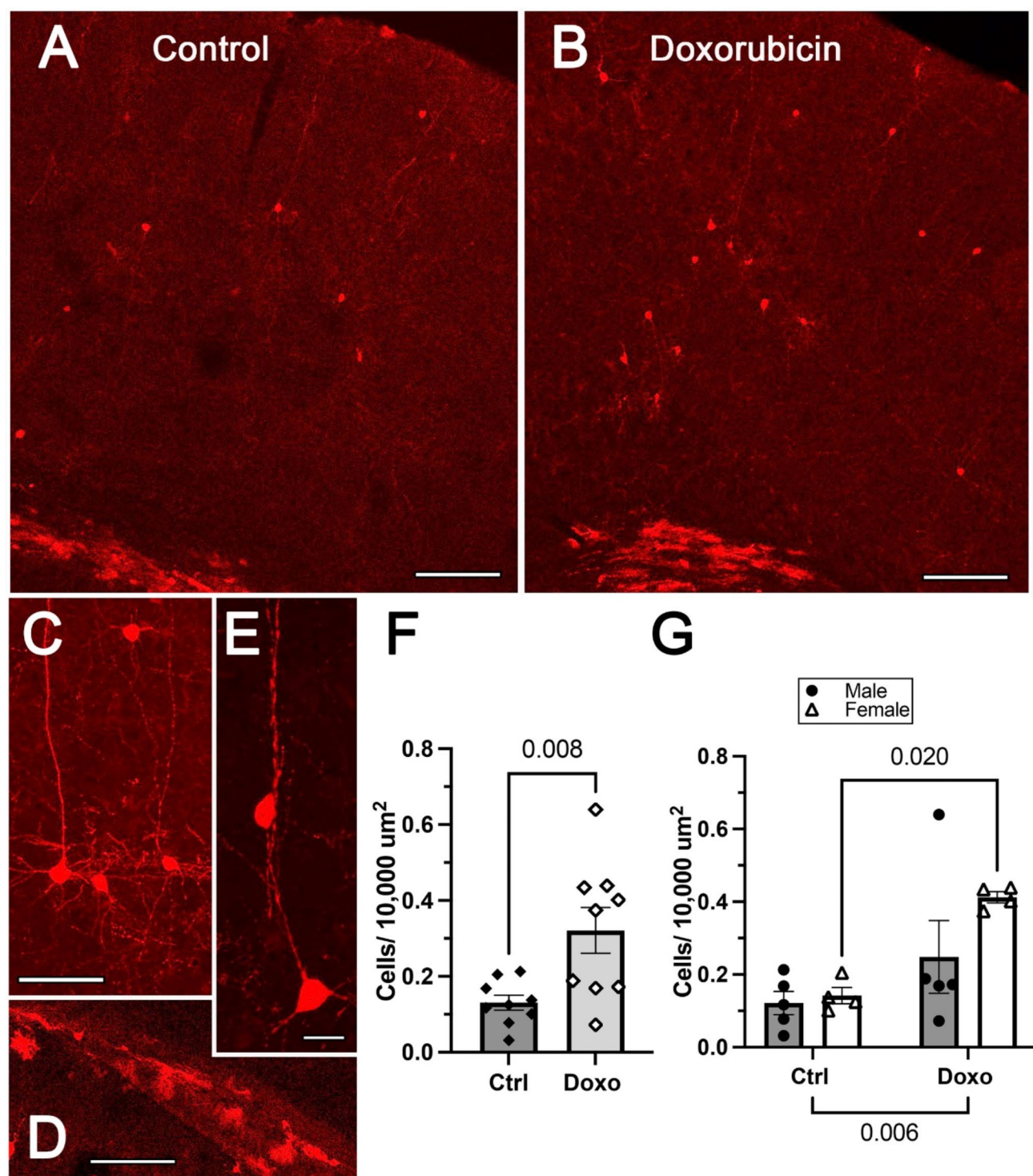


Fig. 6. Doxorubicin increases Ascl1-TdTomato expression in the cortex. **(A)** Representative 10X images of the cerebral cortex region analyzed in a control mouse and **(B)** is a doxorubicin-treated mouse (Magnification bar = 100 μm). **(C–D)** 20X images of Ascl1-TdTomato-positive cells (Magnification bar = 50 μm). **(E)** 40X images of Ascl1-TdTomato-positive cells (Magnification bar = 12 μm). **(F–G)** Quantification based on number of TdTomato-positive cells. Unpaired T-tests and Two-way ANOVAs used to assess outcomes from doxorubicin and sex. Bar graphs represent the mean \pm SEM, $n=4$ –5 animals per group, ~ 4 slices per brain, ~ 3 images at 10x magnification per slice.

of self-renewing capacity in neural cells⁴⁸, heightened Ascl1 levels, in concert with other factors, may drive cell cycle exit and premature exhaustion of the available quiescent stem cells^{43–45}. Thus, our data suggest that doxorubicin induced Ascl1 upregulation could contribute to long-term hippocampal dysfunction in CRCI.

While our study prioritized characterization of Ascl1-mediated neural stem cell proliferation of the subgranular zone, it is noteworthy that Ascl1 is key factor in coordinating gliogenesis, regulating cell cycle re-entry and exit, and driving cell fate reprogramming^{31,33,35,43,49}. There are several conditions that lead to the increased proliferation and development of CNS brain stem cells. Increases to adult neurogenesis and oligodendrogenesis occur from neural stem cell populations as a response to CNS injuries, including ischemia⁵⁰ and experimental autoimmune encephalomyelitis⁵¹. Increases to adult neurogenesis also occur in the olfactory epithelium as a result of acute inflammation⁵². Conversely, intense or prolonged inflammation impairs the generation of new CNS cells⁵³, such as in models of lipopolysaccharide exposure^{54,55}, chronic intestinal inflammation⁵⁶, and diabetes⁵⁷. Doxorubicin increases peripheral inflammation⁵⁸ and brain inflammation^{59,60}. The effects of inflammation on neural stem cell proliferation are partially mediated by growth factors such as brain-derived growth factor and regulation of the transcription factors studied in our work^{53,61}. Consistent with the possibility of bidirectional modulation of neural stem cell proliferation by inflammatory processes, in vitro administration of TNF- α either induced neurogenesis⁶² or apoptosis⁶³, depending on exposure conditions. Thus, the level and timing of neuroinflammation in response to chemotherapy agent may be critical factors in the difference between acutely inducing or chronically inhibiting Ascl1 throughout the brain and in cell stems⁶⁴.

Ascl1 is associated in cancer studies with cell proliferation and pathogenesis^{33,65–67}. Ascl1 hyperactivity has been correlated with conferring drug resistance in cancer cells, including doxorubicin resistance in breast cancer^{66,68,69}. While we did not investigate cancer-Ascl1 dynamics, these observations suggest that cancer and chemotherapy treatment may induce a peripheral upregulation of Ascl1 with downstream effects on hippocampal dysfunction.

While we rigorously assessed the impact of chemotherapy on Ascl1 expression, there are several limitations to consider. Our study prioritized the effects of a single dose of doxorubicin 14 days after treatment in order to assess the short-term alterations; we did not investigate the alterations at other time points or after multi-dose regimens. While results suggested that doxorubicin upregulation of Ascl1 and neural proliferation markers may be greater in female than male mice, the numbers per sex per group (4–5) limited the power for those comparisons. As CRCI symptoms are commonly observed in breast cancer survivors, further investigation of sex effects would be important^{70,71}.

In conclusion, doxorubicin robustly increased Ascl1 expression across the hippocampus and the cerebral cortex. In the dentate gyrus subgranular zone, increases were seen in all subsequent stages of neural stem cell proliferation, demonstrating effects of doxorubicin not only on the exiting of stem cells from quiescence but also on their subsequent development. Chronically, alterations to neural stem cells may contribute to early neural alterations that produce neurogenic depletion, and the cognitive dysfunction as seen in long term effects of CRCI. The strength of these responses also demonstrates that Ascl1 is a good marker of early changes due to peripheral damage caused by doxorubicin; measures of Ascl1 (such as these Ascl1-CreERT2:ROSA mice) would be simple assays for testing the usefulness of agents protective against brain changes relevant to CRCI.

Methods

The experiments performed were performed in accordance with the guidelines and regulations of Public Health Service Policy on Humane Care and Use of Laboratory Animals, and comply with guidelines set forth in the *Guide for the Care and Use of Laboratory Animals*. They were approved by the Georgetown University Institutional Animal Care and Use Committee. All methods are reported in accordance with ARRIVE guidelines.

Ascl1-CreERT2 mice: doxorubicin and tamoxifen treatment

We used Ascl1-CreERT2 mice (generated by OZgene Pty Ltd, Australia) crossed with TdTomato ROSA reporter mice (B6.Cg-Gt(ROSA)26Sor^{tm14(CAG-tdTomato)Hze}/J; strain #007914 obtained from Jackson Labs, Bar Harbor, ME). Both mouse lines were on a C57BL/6 background. In the presence of tamoxifen, the TdTomato fluorescent marker is expressed in conjunction with the Ascl1 promoter. Persistent TdTomato labeling of Ascl1 lineage cells remains up to 180 days post treatment^{36,47}, allowing the evaluation of Ascl1 expression levels from the time of tamoxifen administration.

Five to six-month old Ascl1-CreERT2:ROSA mice were randomly chosen for treatment with either 10 mg/kg doxorubicin or DMSO control ($n=9$ per group, $n=4–5$ per sex, average weights: 31.0 g for control group and 31.3 for treatment group). Doxorubicin hydrochloride (Sigma) was prepared in ultrapure DMSO; 30 μ l of a 20mM solution was diluted to 500 μ l in sterile phosphate-buffered saline and administered via intraperitoneal injection (IP). One week later both treatment groups received IP injections of tamoxifen for four consecutive days⁷². Tamoxifen was dissolved in heated corn oil at 20 mg/mL and delivered at a dose of 60 mg/kg/day. Two weeks after the doxorubicin injection (4 days after the last tamoxifen treatment), mice were euthanized by CO₂ inhalation and perfused with phosphate-buffered saline (Fig. 1A). At euthanasia, the doxorubicin- and tamoxifen-treated mice had lost more weight than the control mice treated only with tamoxifen, as expected (11.8% versus 6.5%). Brains were collected, fixed in 4% Formalin/ 4% sucrose, and transitioned through a sucrose gradient. Fixed brains were flash frozen and sliced coronally at 30 μ m for immunohistochemistry.

Immunohistochemistry

For blocking, sections were washed with Tris-buffered saline (TBS) and blocked in TBS plus 0.3% Triton X (TBS-X) with either bovine serum albumin, donkey serum, or normal goat serum, depending on the antibody used (Supplemental Table 1). The TdTomato expression from the Ascl1 promoter was visualized using anti-red fluorescent protein (RFP) antibodies in all immunostains. The anti-RFP antibody was used in conjunction with

antibodies for different stages of neurogenesis: Sox2, NeuroD1, or GFAP. Antibodies were incubated on tissue sections overnight at 4 °C. Sections were incubated with secondary antibodies for cell visualization, then cell nuclei identified with DAPI (1:10,000 dilution). The sources of antibodies used are described in Supplemental Table 2.

Imaging and analysis

Fluorescent imaging was performed with a Zeiss Axio Imager 2 microscope at 10X or 20X magnification. All immunostains were visualized using Alexa Fluor secondary antibodies, with the excitation of anti-RFP captured at 594 nm wavelengths (red) and all other antibodies at 488 nm (green). Blinded analysis with ImageJ was performed in all immunostains. For hippocampal analyses, approximately 4 slices were analyzed for each mouse brain. Within each section, regions of interest (ROIs) were drawn around the area of the dentate gyrus using the DAPI channel (460 nm) to define its area between 100,000 and 150,000 μm^2 . All subsequent measurements were normalized to the exact dentate gyrus area, following a conversion scale of 2.90 pixels/micron for 10X images and 5.80 pixels/micron for 20X images.

For Ascl1-TdTomato measures, approximately three 20X images per slice were collected at approximately 60 millisecond (ms) exposure times to capture the entire dentate gyrus area. The ROIs of the dentate gyrus were then superimposed onto the TdTomato (RFP-positive) images and the number of TdTomato cells was manually counted in a blinded manner using the ImageJ point tool. Only RFP-positive cells along the dentate gyrus subgranular zone were counted. Cells lacking a clear cell body and neuronal cells out of the subgranular zone were excluded from the count. Mean intensity was measured, controlling for background intensity by subtracting the average of three mean intensity recordings. After thresholding, the percent area coverage of RFP-positive cells was measured.

For the Sox2 (green) and RFP (red) co-stains, the dentate gyrus ROIs were drawn and superimposed over 10X composite images of Sox2 captured at 700ms exposure times and RFP at 180ms (one image per brain slice). Within the granule cell layer of the dentate gyrus, colocalization of the green and red cells were manually counted using the ImageJ point tool. Colocalization was characterized by bright fluorescent yellow color in the cell bodies, indicating expression of Sox2 within the RFP-positive cells. Any overlapping cells or cells lacking a clear cell body were excluded from the count. Thresholding was performed to measure percent area coverage of Sox2 expression alone. The ROIs were then superimposed on the Sox2 channel and percent area coverage was recorded. In addition, the total number of all cells expressing Sox2 were counted from the same images in the region of the hippocampus that contained the RFP-positive cells.

For the NeuroD1 (green) and RFP (red) co-stains, the same protocol was used on approximately three 20X images per slice with NeuroD1 captured at 650ms exposure times and RFP at 60ms. The number of yellow colocalized cells was quantified. The NeuroD1 channel was thresholded and percent area coverage of NeuroD1 expression within the dentate gyrus was recorded.

For GFAP and RFP co-stains, ROIs of the dentate gyrus were again drawn and superimposed over 20X composite images of GFAP (green) captured at 600ms exposure times and RFP (red) captured at 100ms. The total number of cells with yellow colocalization was manually counted within the dentate gyrus. In contrast to other cell counts, cells with colocalized processes were separately counted to assess the radial glial cells (Type 1 progenitors). Type 1 progenitors were characterized by bright fluorescent yellow color in a single cell process extending from the cell body. Cells with colocalization in the cell body alone, lacking yellow cell processes, were excluded from the analysis. Mean intensity of GFAP expression in the dentate gyrus was measured, controlling for background intensity by subtracting the average of three mean intensity recordings.

For the cerebral cortex, TdTomato expression was assessed using the average of three 10X images per slice. ROIs were drawn to measure the entire depth of the neocortex dorsal to the hippocampus, excluding all non-cortical areas. RFP-positive cells were manually counted. The density of cells per cortical area were calculated. A Zeiss LSM 880 confocal microscope was used for the collection of representative 10X, 20X and 40X images.

All statistical analysis was performed with GraphPad Prism 10. Two-way ANOVAS with Sidak's multiple comparison test and unpaired T-tests were used to assess outcome measures from doxorubicin treatment and sex of 9 treated and 9 untreated mice. Brain samples from all mice were included in the analyses. After initial analyses, groups were split between males ($n = 5$) and females ($n = 4$). All results were calculated per area assessed. Results of cell counts were reported as cells per 10,000 μm^2 .

Data availability

The data generated in this study are available upon request from the corresponding author.

Received: 12 January 2025; Accepted: 13 March 2025

Published online: 21 March 2025

References

1. Demos-Davies, K., Lawrence, J. & Seelig, D. Cancer related cognitive impairment: a downside of cancer treatment. *Front. Oncol.* **14**, 1387251 (2024).
2. Winocur, G., Johnston, I. & Castel, H. Chemotherapy and cognition: international cognition and cancer task force recommendations for harmonising preclinical research. *Cancer Treat. Rev.* **69**, 72–83 (2018).
3. Jansen, C. E., Miaskowski, C., Dodd, M., Dowling, G. & Kramer, J. A metaanalysis of studies of the effects of cancer chemotherapy on various domains of cognitive function. *Cancer* **104** (10), 2222–2233 (2005).
4. Fernandez, H. R., Varma, A., Flowers, S. A. & Rebeck, G. W. Cancer chemotherapy related cognitive impairment and the impact of the Alzheimer's disease risk factor APOE. *Cancers (Basel)* **12** (12), E3842 (2020).
5. Murillo, L. C., Sutachan, J. J. & Albarracín, S. L. An update on Neurobiological mechanisms involved in the development of chemotherapy-induced cognitive impairment (CICI). *Toxicol. Rep.* **10**, 544–553 (2023).

6. Mounier, N. M., Abdel-Maged, A. E. S., Wahdan, S. A., Gad, A. M. & Azab, S. S. Chemotherapy-induced cognitive impairment (CICI): an overview of etiology and pathogenesis. *Life Sci.* **258**, 118071 (2020).
7. Yang, M. et al. Cyclophosphamide impairs hippocampus-dependent learning and memory in adult mice: Possible involvement of hippocampal neurogenesis in chemotherapy-induced memory deficits. *Neurobiol. Learn. Mem.* **93** (4), 487–494 (2010).
8. Dietrich, J., Han, R., Yang, Y., Mayer-Pröschel, M. & Noble, M. CNS progenitor cells and oligodendrocytes are targets of chemotherapeutic agents in vitro and in vivo. *J. Biol.* **5** (7), 22 (2006).
9. Christie, L. A. et al. Impaired cognitive function and hippocampal neurogenesis following cancer chemotherapy. *Clin. Cancer Res.* **18** (7), 1954–1965 (2012).
10. Seigers, R. et al. Neurobiological changes by cytotoxic agents in mice. *Behav. Brain. Res.* **299**, 19–26 (2016).
11. Monje, M. L. et al. Impaired human hippocampal neurogenesis after treatment for central nervous system malignancies. *Ann. Neurol.* **62** (5), 515–520 (2007).
12. Lange, M. et al. Cancer-related cognitive impairment: an update on state of the art, detection, and management strategies in cancer survivors. *Ann. Oncol.* **30** (12), 1925–1940 (2019).
13. Serini, S. & Calviello, G. Potential of natural phenolic compounds against Doxorubicin-Induced chemobrain: Biological and molecular mechanisms involved. *Antioxidants* **13** (4), 486 (2024).
14. Tacar, O., Sriamornsak, P. & Dass, C. R. Doxorubicin: an update on anticancer molecular action, toxicity and novel drug delivery systems. *J. Pharm. Pharmacol.* **65** (2), 157–170 (2013).
15. Dias, G. P. et al. Consequences of cancer treatments on adult hippocampal neurogenesis: Implications for cognitive function and depressive symptoms. *Neuro-Oncology* **16** (4), 476 (2014).
16. Jaiswara, P. K. & Shukla, S. K. Chemotherapy-mediated neuronal aberration. *Pharmaceuticals (Basel)* **16** (8), 1165 (2023).
17. Abbott, L. C. & Nigussie, F. Adult neurogenesis in the mammalian dentate gyrus. *Anat. Histol. Embryol.* **49** (1), 3–16 (2020).
18. Urbán, N. & Guillemot, F. Neurogenesis in the embryonic and adult brain: Same regulators, different roles. *Front. Cell. Neurosci.* **8**, 396 (2014).
19. Terreros-Roncal, J. et al. Methods to study adult hippocampal neurogenesis in humans and across the phylogeny. *Hippocampus* **33** (4), 271–306 (2023).
20. Llorens-Martin, M., Rábano, A. & Ávila, J. The Ever-Changing morphology of hippocampal granule neurons in physiology and pathology. *Front. Neurosci.* **9**, 526 (2016).
21. Sekeres, M. J., Bradley-Garcia, M., Martinez-Canabal, A. & Winocur, G. Chemotherapy-Induced cognitive impairment and hippocampal neurogenesis: A review of physiological mechanisms and interventions. *Int. J. Mol. Sci.* **22** (23), 12697 (2021).
22. Dias-Carvalho, A. et al. Four decades of chemotherapy-induced cognitive dysfunction: Comprehensive review of clinical, animal and in vitro studies, and insights of key initiating events. *Arch. Toxicol.* **96** (1), 11–78 (2022).
23. El-Agamy, S. E., Abdel-Aziz, A. K., Esmat, A. & Azab, S. S. Chemotherapy and cognition: Comprehensive review on doxorubicin-induced chemobrain. *Cancer Chemother. Pharmacol.* **84** (1), 1–14 (2019).
24. Nguyen, L. D. & Ehrlich, B. E. Cellular mechanisms and treatments for chemobrain: Insight from aging and neurodegenerative diseases. *EMBO Mol. Med.* **12** (6), e12075 (2020).
25. Du, J. et al. Doxorubicin-Induced cognitive impairment: The mechanistic insights. *Front. Oncol.* **11**, 673340 (2021).
26. Janelins, M. C. et al. IGF-1 partially restores chemotherapy-induced reductions in neural cell proliferation in adult C57BL/6 mice. *Cancer Invest.* **28** (5), 544–553 (2010).
27. Park, H. S. et al. Physical exercise prevents cognitive impairment by enhancing hippocampal neuroplasticity and mitochondrial function in doxorubicin-induced chemobrain. *Neuropharmacology* **133**, 451–461 (2018).
28. Kitamura, Y. et al. Doxorubicin and cyclophosphamide treatment produces anxiety-like behavior and Spatial cognition impairment in rats: possible involvement of hippocampal neurogenesis via brain-derived neurotrophic factor and Cyclin D1 regulation. *Behav. Brain. Res.* **292**, 184–193 (2015).
29. Ghosh, H. S. Adult neurogenesis and the promise of adult neural stem cells. *J. Exp. Neurosci.* **13**, 1179069519856876 (2019).
30. Beckervordersandforth, R., Zhang, C. L. & Lie, D. C. Transcription-factor-dependent control of adult hippocampal neurogenesis. *Cold Spring Harb Perspect. Biol.* **7** (10), a018879 (2015).
31. Andersen, J. et al. A transcriptional mechanism integrating inputs from extracellular signals to activate hippocampal stem cells. *Neuron* **83** (5), 1085–1097 (2014).
32. Castro, D. S. et al. A novel function of the proneural factor Ascl1 in progenitor proliferation identified by genome-wide characterization of its targets. *Genes Dev.* **25** (9), 930–945 (2011).
33. Parkinson, L. M. et al. The proneural transcription factor ASCL1 regulates cell proliferation and primes for differentiation in neuroblastoma. *Front. Cell. Dev. Biol.* **10**, 942579 (2022).
34. Raposo, A. A. S. F. et al. Ascl1 coordinately regulates gene expression and the chromatin landscape during neurogenesis. *Cell. Rep.* **10** (9), 1544–1556 (2015).
35. Kim, E. J., Leung, C. T., Reed, R. R. & Johnson, J. E. In vivo analysis of Ascl1 defined progenitors reveals distinct developmental dynamics during adult neurogenesis and gliogenesis. *J. Neurosci.* **27** (47), 12764–12774 (2007).
36. Kim, E. J., Ables, J. L., Dickel, L. K., Eisch, A. J. & Johnson, J. E. Ascl1 (Mash1) defines cells with Long-Term neurogenic potential in subgranular and subventricular zones in adult mouse brain. *PLoS One* **6** (3), e18472 (2011).
37. Berg, D. A., Bond, A. M., Ming, G. & Li, Song, H. Radial glial cells in the adult dentate gyrus: What are they and where do they come from? F1000Research (2018). <https://f1000research.com/articles/7-277>. Accessed 23 Sep 2024.
38. Gonçalves, J. T., Schafer, S. T. & Gage, F. H. Adult neurogenesis in the hippocampus: From stem cells to behavior. *Cell* **167** (4), 897–914 (2016).
39. Oproescu, A. M., Han, S. & Schuurmans, C. New insights into the intricacies of proneural gene regulation in the embryonic and adult cerebral cortex. *Front. Mol. Neurosci.* **14**, 642016 (2021).
40. Vainorius, G. et al. Ascl1 and Ngn2 convert mouse embryonic stem cells to neurons via functionally distinct paths. *Nat. Commun.* **14**, 5341 (2023).
41. Ghazale, H. et al. Ascl1 phospho-site mutations enhance neuronal conversion of adult cortical astrocytes in vivo. *Front. Neurosci.* **16**, 917071 (2022).
42. Nakatani, H. et al. Ascl1/Mash1 promotes brain oligodendrogenesis during myelination and remyelination. *J. Neurosci.* **33** (23), 9752–9768 (2013).
43. Wapinski, O. L. et al. Hierarchical mechanisms for transcription factor-mediated reprogramming of fibroblasts to neurons. *Cell* **155** (3). <https://doi.org/10.1016/j.cell.2013.09.028> (2013).
44. Woods, L. M. et al. Elevated ASCL1 activity creates de Novo regulatory elements associated with neuronal differentiation. *BMC Genom.* **23**, 255 (2022).
45. Sueda, R., Imai, Y., Harima, Y. & Kageyama, R. High Hes1 expression and resultant Ascl1 suppression regulate quiescent versus active neural stem cells in the adult mouse brain. *Genes Dev.* **33** (9–10), 511–523 (2019).
46. Bigotte, L., Arvidson, B. & Olsson, Y. Cytofluorescence localization of adriamycin in the nervous system. I. Distribution of the drug in the central nervous system of normal adult mice after intravenous injection. *Acta Neuropathol.* **57** (2–3), 121–129 (1982).
47. Yang, S. M., Alvarez, D. D. & Schinder, A. F. Reliable genetic labeling of Adult-Born dentate granule cells using Ascl1CreERT2 and GlastCreERT2 murine lines. *J. Neurosci.* **35** (46), 15379–15390 (2015).
48. Park, N. I. et al. ASCL1 reorganizes chromatin to direct neuronal fate and suppress tumorigenicity of glioblastoma stem cells. *Cell. Stem Cell.* **21** (2), 209–224e7 (2017).

49. Sueda, R. & Kageyama, R. Regulation of active and quiescent somatic stem cells by Notch signaling. *Dev. Growth Differ.* **62** (1), 59–66 (2020).
50. Kokaia, Z. & Lindvall, O. Neurogenesis after ischaemic brain insults. *Curr. Opin. Neurobiol.* **13** (1), 127–132 (2003).
51. Picard-Riera, N. et al. Experimental autoimmune encephalomyelitis mobilizes neural progenitors from the subventricular zone to undergo oligodendrogenesis in adult mice. *Proc. Natl. Acad. Sci. U S A.* **99** (20), 13211–13216 (2002).
52. Chen, M., Reed, R. R. & Lane, A. P. Acute inflammation regulates neuroregeneration through the NF- κ B pathway in olfactory epithelium. *Proc. Natl. Acad. Sci. U S A.* **114** (30), 8089–8094 (2017).
53. Chesnokova, V., Pechnick, R. N. & Wawrowsky, K. Chronic peripheral inflammation, hippocampal neurogenesis, and behavior. *Brain Behav. Immun.* **58**, 1–8 (2016).
54. Ekdahl, C. T., Claasen, J. H., Bonde, S., Kokaia, Z. & Lindvall, O. Inflammation is detrimental for neurogenesis in adult brain. *Proc. Natl. Acad. Sci. U S A.* **100** (23), 13632–13637 (2003).
55. Monje, M. L., Toda, H. & Palmer, T. D. Inflammatory Blockade restores adult hippocampal neurogenesis. *Science* **302** (5651), 1760–1765 (2003).
56. Zonis, S. et al. Chronic intestinal inflammation alters hippocampal neurogenesis. *J. Neuroinflammation* **12**, 65 (2015).
57. Ho, N., Sommers, M. S. & Lucki, I. Effects of diabetes on hippocampal neurogenesis: Links to cognition and depression. *Neurosci. Biobehav. Rev.* **37** (8), 1346–1362 (2013).
58. Budamagunta, V. et al. Senolytic treatment alleviates doxorubicin-induced chemobrain. *Aging Cell.* **23** (2), e14037 (2024).
59. Savran, M. et al. Agomelatine ameliorates doxorubicin-induced cortical and hippocampal brain injury via Inhibition of TNF- α /NF- κ B pathway. *Toxicol. Mech. Methods* **34** (4), 359–368 (2024).
60. Alhowail, A. H. Pioglitazone ameliorates DOX-induced cognitive impairment by mitigating inflammation, oxidative stress, and apoptosis of hippocampal neurons in rats. *Behav. Brain. Res.* **457**, 114714 (2024).
61. Shohayeb, B., Diab, M., Ahmed, M. & Ng, D. C. H. Factors that influence adult neurogenesis as potential therapy. *Transl. Neurodegener.* **7**, 4 (2018).
62. Bernardino, L. et al. Tumor necrosis factor- α modulates survival, proliferation, and neuronal differentiation in neonatal subventricular zone cell cultures. *Stem Cells* **26** (9), 2361–2371 (2008).
63. Sheng, W. S. et al. TNF- α -induced chemokine production and apoptosis in human neural precursor cells. *J. Leukoc. Biol.* **78** (6), 1233–1241 (2005).
64. Whitney, N. P., Eidem, T. M., Peng, H., Huang, Y. & Zheng, J. C. Inflammation mediates varying effects in neurogenesis: Relevance to the pathogenesis of brain injury and neurodegenerative disorders. *J. Neurochem.* **108** (6), 1343–1359 (2009).
65. Nie, J., Zhang, P., Liang, C., Yu, Y. & Wang, X. ASCL1-mediated ferroptosis resistance enhances the progress of castration-resistant prostate cancer to neurosecretory prostate cancer. *Free Radic Biol. Med.* **205**, 318–331 (2023).
66. Li, Y. et al. Identification of molecular subtypes based on chromatin regulator-related genes and experimental verification of the role of ASCL1 in conferring chemotherapy resistance to breast cancer. *Front. Immunol.* **15** (2024). <https://www.frontiersin.org/journals/immunology/articles/https://doi.org/10.3389/fimmu.2024.1390261/full>. Accessed 10 Dec 2024.
67. Rheinbay, E. et al. An aberrant transcription factor network essential for Wnt signaling and stem cell maintenance in glioblastoma. *Cell. Rep.* **3** (5), 1567–1579 (2013).
68. Nouruzi, S. et al. ASCL1 activates neuronal stem cell-like lineage programming through remodeling of the chromatin landscape in prostate cancer. *Nat. Commun.* **13** (1), 2282 (2022).
69. Hu, B. et al. ASCL1 drives tolerance to osimertinib in EGFR mutant lung cancer in permissive cellular contexts. *Cancer Res.* **84** (8), 1303–1319 (2024).
70. Zhou, X. et al. Prevalence and associated factors of chemotherapy-related cognitive impairment in older breast cancer survivors. *J. Adv. Nurs.* **80** (2), 484–499 (2024).
71. Jim, H. S. L. et al. Meta-analysis of cognitive functioning in breast cancer survivors previously treated with standard-dose chemotherapy. *J. Clin. Oncol.* **30** (29), 3578–3587 (2012).
72. Silbereis, J., Cheng, E., Ganat, Y. M., Ment, L. R. & Vaccarino, F. M. Precursors with GFAP promoter activity transiently generate GABA interneurons in the postnatal cerebellum. *Stem Cells* **27** (5), 1152–1163 (2009).

Acknowledgements

This work was supported by NIH grants R01AG071745 (GWR) and R35CA283926 (JM). This research was also supported in part by R01AG082348 (JM). Fellowship funding (MP) was provided by American Cancer Society Diversity in Cancer Research award DICR INTR-23-1253711-01-DICR INTR.

Author contributions

C.A.N. was responsible for designing and conducting experiments, interpreting results, and writing the manuscript. M.P. and M.F.L. were responsible for conducting experiments and editing the manuscript. L.F. and J.M. were responsible for developing the scientific ideas and editing the manuscript. G.W.R. was responsible for designing experiments and editing the manuscript.

Declarations

Competing interests

The authors declare no competing interests.

Additional information

Supplementary Information The online version contains supplementary material available at <https://doi.org/10.1038/s41598-025-94400-8>.

Correspondence and requests for materials should be addressed to G.W.R.

Reprints and permissions information is available at www.nature.com/reprints.

Publisher's note Springer Nature remains neutral with regard to jurisdictional claims in published maps and institutional affiliations.

Open Access This article is licensed under a Creative Commons Attribution-NonCommercial-NoDerivatives 4.0 International License, which permits any non-commercial use, sharing, distribution and reproduction in any medium or format, as long as you give appropriate credit to the original author(s) and the source, provide a link to the Creative Commons licence, and indicate if you modified the licensed material. You do not have permission under this licence to share adapted material derived from this article or parts of it. The images or other third party material in this article are included in the article's Creative Commons licence, unless indicated otherwise in a credit line to the material. If material is not included in the article's Creative Commons licence and your intended use is not permitted by statutory regulation or exceeds the permitted use, you will need to obtain permission directly from the copyright holder. To view a copy of this licence, visit <http://creativecommons.org/licenses/by-nc-nd/4.0/>.

© The Author(s) 2025